

NASA TECHNICAL NOTE



NASA TN D-4382

NASA TN D-4382

2.1

LOAN COPY: RET  
AFWL (WLIL)  
KIRTLAND AFB, I.

0131450



TECH LIBRARY KAFB, NM

# AERODYNAMIC EVALUATION OF TWO-STAGE AXIAL-FLOW TURBINE DESIGNED FOR BRAYTON-CYCLE SPACE POWER SYSTEM

by Milton G. Kofskey and William J. Nusbaum

Lewis Research Center  
Cleveland, Ohio

NATIONAL AERONAUTICS AND SPACE ADMINISTRATION • WASHINGTON, D. C. • FEBRUARY 1968

TECH LIBRARY KAFB, NM



0131450

AERODYNAMIC EVALUATION OF TWO-STAGE AXIAL-FLOW TURBINE  
DESIGNED FOR BRAYTON-CYCLE SPACE POWER SYSTEM

By Milton G. Kofskey and William J. Nusbaum

Lewis Research Center  
Cleveland, Ohio

NATIONAL AERONAUTICS AND SPACE ADMINISTRATION

---

For sale by the Clearinghouse for Federal Scientific and Technical Information  
Springfield, Virginia 22151 — CFSTI price \$3.00

# AERODYNAMIC EVALUATION OF TWO-STAGE AXIAL-FLOW TURBINE DESIGNED FOR BRAYTON-CYCLE SPACE POWER SYSTEM

by Milton G. Kofskey and William J. Nusbaum

Lewis Research Center

## SUMMARY

An experimental investigation was conducted of a two-stage turbine designed to drive an alternator for a 10-kilowatt-shaft-output space power system. First-stage and two-stage performance results are described for operation at approximately design Reynolds number at equivalent design speed and pressure ratio with argon as the working fluid. Tests were made at speeds ranging from 0 to 120 percent of equivalent design speed and at pressure ratios from 1.02 to 1.65.

The results of the investigation indicated that, for two-stage operation, the static and total efficiencies, based on turbine-inlet and rotor-exit conditions, were 0.825 and 0.845, respectively, which compare favorably with design. The equivalent mass flow, however, was 4 percent lower than design and was attributed to the flow areas in the blade rows being smaller than design. At this point the first- and second-stage total efficiencies were 0.864 and 0.805 or approximately 2 points higher and 4 points lower than design, respectively. As a result, the stage work split was indicated to be 53 to 47 compared with a design equal split.

Two-stage performance based on turbine-inlet and collector-exit conditions indicated static and total efficiencies of 0.826 and 0.835, respectively. These results, which indicate a drop in total efficiency within the collector of approximately 1 point with no change in static efficiency, compare closely with design.

## INTRODUCTION

NASA is currently investigating components of a Brayton-cycle space power system with a 10-kilowatt-shaft power output. The reference system, described in reference 1, is of the two-shaft arrangement wherein one turbine drives the compressor and another turbine drives the alternator. This arrangement was selected because of the large

difference in speed requirements between the compressor and the alternator and because of problems associated with the use of a speed-reduction gearbox. Rotative speeds in the range of 30 000 to 50 000 rpm are required in order to obtain high compressor efficiency with a minimum number of stages. The speed of the alternator is comparatively low at 12 000 rpm because of the system frequency requirement of 400 cycles per second. Therefore, use of the two-shaft arrangement would permit both the compressor and alternator to operate at their optimum rotative speeds without the use of a speed-reduction gearbox.

Cold-performance evaluations have been made on a radial-inflow turbine designed to drive the high-speed compressor used in this reference system. Results of these investigations, as reported in references 2 and 3, indicated that efficiencies in the 85- to 90-percent range can be obtained for the compressor-drive turbine.

A two-stage axial-flow turbine with a mean diameter of 8.5 inches (21.59 cm) was designed to drive the alternator. The turbine was designed and fabricated under contract, and a description of the design and mechanical testing of the turbine by the contractor is given in reference 4.

Results of Reynolds number investigations using axial-flow turbines show that the turbine efficiency level is dependent on Reynolds number. For example, the results of reference 5 show a 5-point decrease in turbine efficiency when the Reynolds number was decreased from  $1.2 \times 10^6$  to  $1.08 \times 10^5$ . Since the subject alternator turbine was designed to operate at a Reynolds number of  $4.95 \times 10^4$ , which is substantially lower than that normally encountered, it was considered important to establish the performance characteristics of this turbine at these low-Reynolds-number conditions.

Accordingly, an experimental investigation of the two-stage turbine was made at Lewis to determine the overall and stage performance of this unit. The turbine package used conventional oil-lubricated bearings to simplify the performance tests, instead of the gas bearings which would be used for the space power system.

Turbine performance tests were made with argon as the working fluid at an inlet temperature of  $610^\circ R$  ( $339^\circ K$ ) and at an inlet pressure of 2.5 psia ( $1.723 \text{ newtons/cm}^2$ ) to correspond to design Reynolds number at design speed and pressure ratio. Data were obtained over a range of total- to static-pressure ratios of 1.02 to 1.65 and over a range of speeds from 0 to 120 percent of design value.

This report presents design information and turbine performance for first-stage and two-stage operation. Test results are presented in terms of equivalent specific work, torque, mass flow, and efficiency. A radial survey of rotor-exit flow angle and total pressure is also presented for both first-stage and two-stage operation.

## TURBINE DESCRIPTION

As mentioned in the INTRODUCTION, the two-stage axial-flow turbine was designed to drive a low-speed alternator for a 10-kilowatt-shaft-output space power system with argon as the working fluid. A detailed description of the aerodynamic and mechanical design of this turbine is given in reference 4. For convenience, the more important design values and turbine features are presented herein. The design point values are

TABLE I. - TURBINE DESIGN VALUES

	Operation	
	First-stage	Two-stage
Design point (argon)		
Inlet total temperature, $T_1'$ , $^{\circ}\text{R}$ ( $^{\circ}\text{K}$ )	1685 (936.11)	1685 (936.11)
Inlet total pressure, $p_1'$ , psia (newtons/cm $^2$ )	8.45 (5.826)	8.45 (5.826)
Mass flow, $w$ , lb/sec (kg/sec)	0.611 (0.277)	0.611 (0.277)
Turbine rotative speed, $N$ , rpm	12 000	12 000
Total- to static-pressure ratio		
Overall, $p_1'/p_6$	-----	1.2540
Rotor exit, $p_1'/p_3$ or 5	1.1206	1.2542
Total- to total-pressure ratio		
Overall, $p_1'/p_6'$	-----	1.2495
Rotor exit, $p_1'/p_3'$ or 5	1.1144	1.2469
Blade-jet speed ratio, $\nu$	0.651	0.465
Total to static efficiency, $\eta_s$		
Overall	-----	0.826
Rotor exit	0.805	0.825
Total to total efficiency, $\eta_t$		
Overall	-----	0.843
Rotor exit	0.847	0.850
Specific work, $\Delta h$ , Btu/lb (joules/gram)	7.52 (17.505)	15.04 (35.010)
Reynolds number, $Re = w/\mu r_m$	49 500	49 500
Air equivalent		
Mass flow, $\epsilon w \sqrt{\theta_{cr}} / \delta$ , lb/sec (kg/sec)	1.537 (0.697)	1.537 (0.697)
Specific work, $\Delta h/\theta_{cr}$ , Btu/lb (joules/gram)	2.98 (6.937)	5.96 (13.874)
Torque, $\tau \epsilon / \delta$ , in.-lb (newton-meter)	54.06 (6.108)	108.12 (12.216)
Rotative speed, $N/\sqrt{\theta_{cr}}$ , rpm	7554	7554
Total- to total-pressure ratio		
Overall, $p_1'/p_6'$ eq	-----	1.226
Rotor exit, $p_1'/p_3'$ or 5, eq	1.106	1.225
Total- to static-pressure ratio		
Overall, $p_1'/p_6$ , eq	-----	1.232
Rotor exit, $p_1'/p_3$ or 5, eq	1.112	1.233
Blade-jet speed ratio, $\nu$	0.651	0.465

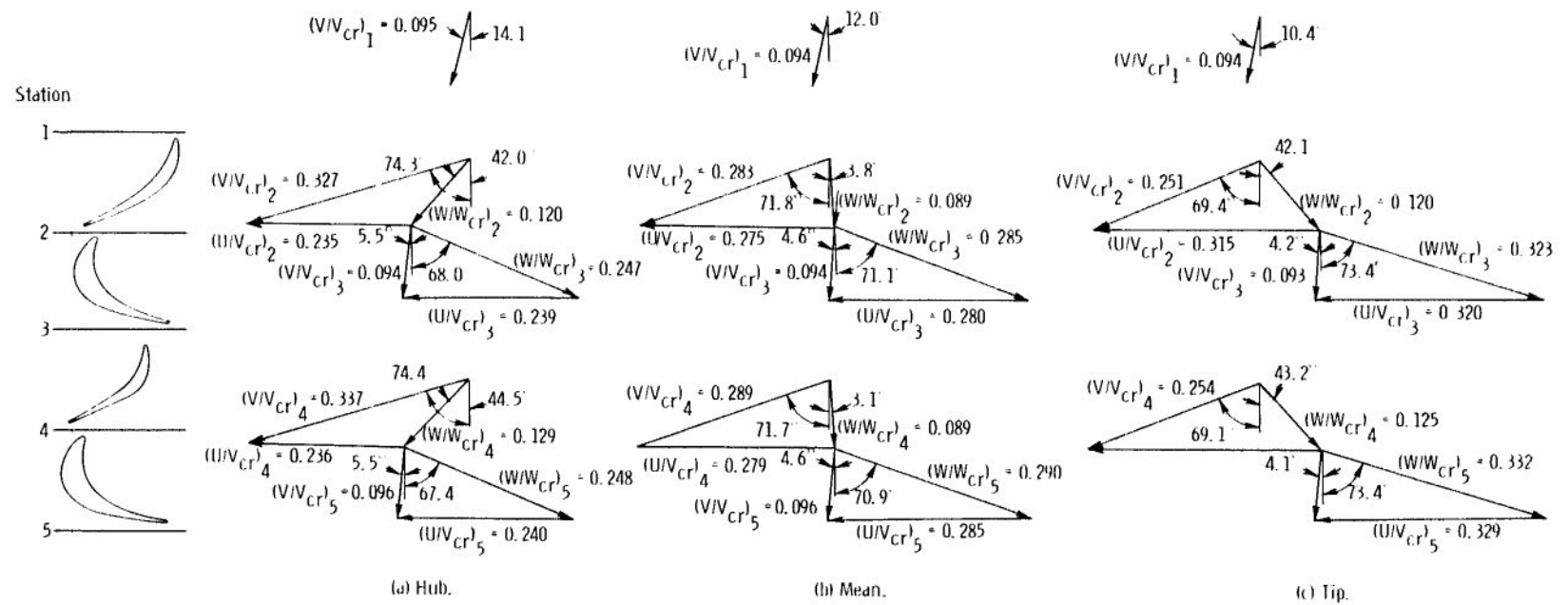


Figure 1. - Design velocity diagrams.

listed in table I. Design-point values are given at design inlet pressure and temperature with argon as the working fluid. Air equivalent values for the design point are also given with the assumption of the same values of efficiency as for argon.

## Velocity Diagrams

From the design conditions of pressure, temperature, weight flow, and speed, velocity diagrams were calculated to meet the design work requirement, with the assumption of an equal work split between the two stages. Values of efficiency which were used in the calculation included the effects of both low Reynolds number and rotor blade tip leakage. The predicted efficiencies were based on loss coefficients which were adjusted in accordance with the 1/5 power law for viscous losses. Velocity diagrams (fig. 1) were calculated at the hub, mean, and tip diameters to give free vortex flow patterns. The diagrams indicate a conservative aerodynamic design with a relatively low level of velocity through both stages. The turning at the mean diameter is  $67.3^{\circ}$  and  $67.8^{\circ}$  for the first- and second-stage rotors, respectively, with a large amount of reaction in both stages. Stator-exit angles of approximately  $72^{\circ}$  at the mean diameter are also quite conservative, in that exit angles of  $75^{\circ}$  or less are usually considered favorable for low blade leaving losses. There is a small amount of turbine-exit whirl in the direction of rotation. Prerotation of the flow at the turbine inlet, as shown in figure 1, simulates that condition which would be established by an axial-flow compressor drive turbine, described in reference 6, which is also part of this technology program.

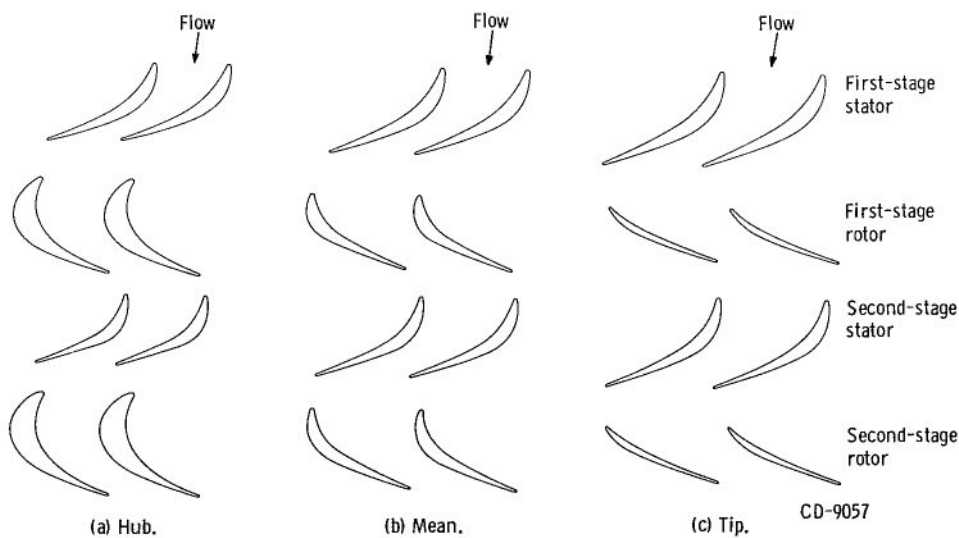


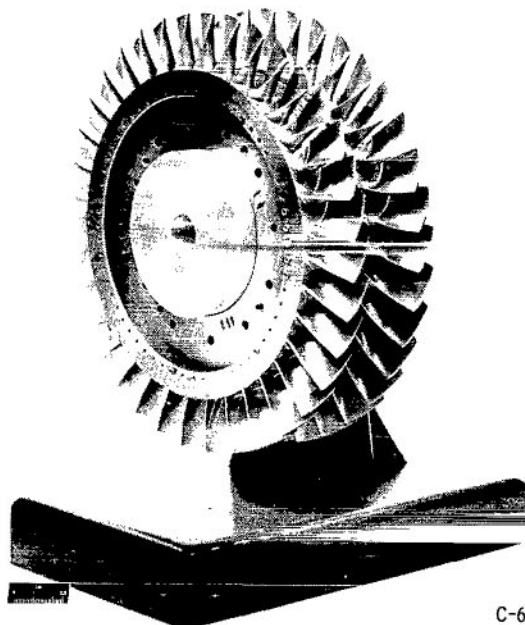
Figure 2. - Stator and rotor blade passages and profiles.

## Stator Blading

The stator design resulted in 44 blades for the first stage and 40 blades for the second stage with respective values of solidity at the mean diameter of 1.57 and 1.56. The stator blade passages and profiles at the hub, mean, and tip diameters are shown in figure 2. The stators are quite conventional with a convergence of the flow passage from the inlet to the throat that results, generally, in accelerating flow in that portion of the passage on both the suction and pressure surfaces. The design blade-surface velocity distributions at the hub, mean, and tip diameters are presented in reference 4. The figures therein show only a small amount of deceleration on the suction surface downstream of the throat and on the pressure surface near the leading edge.

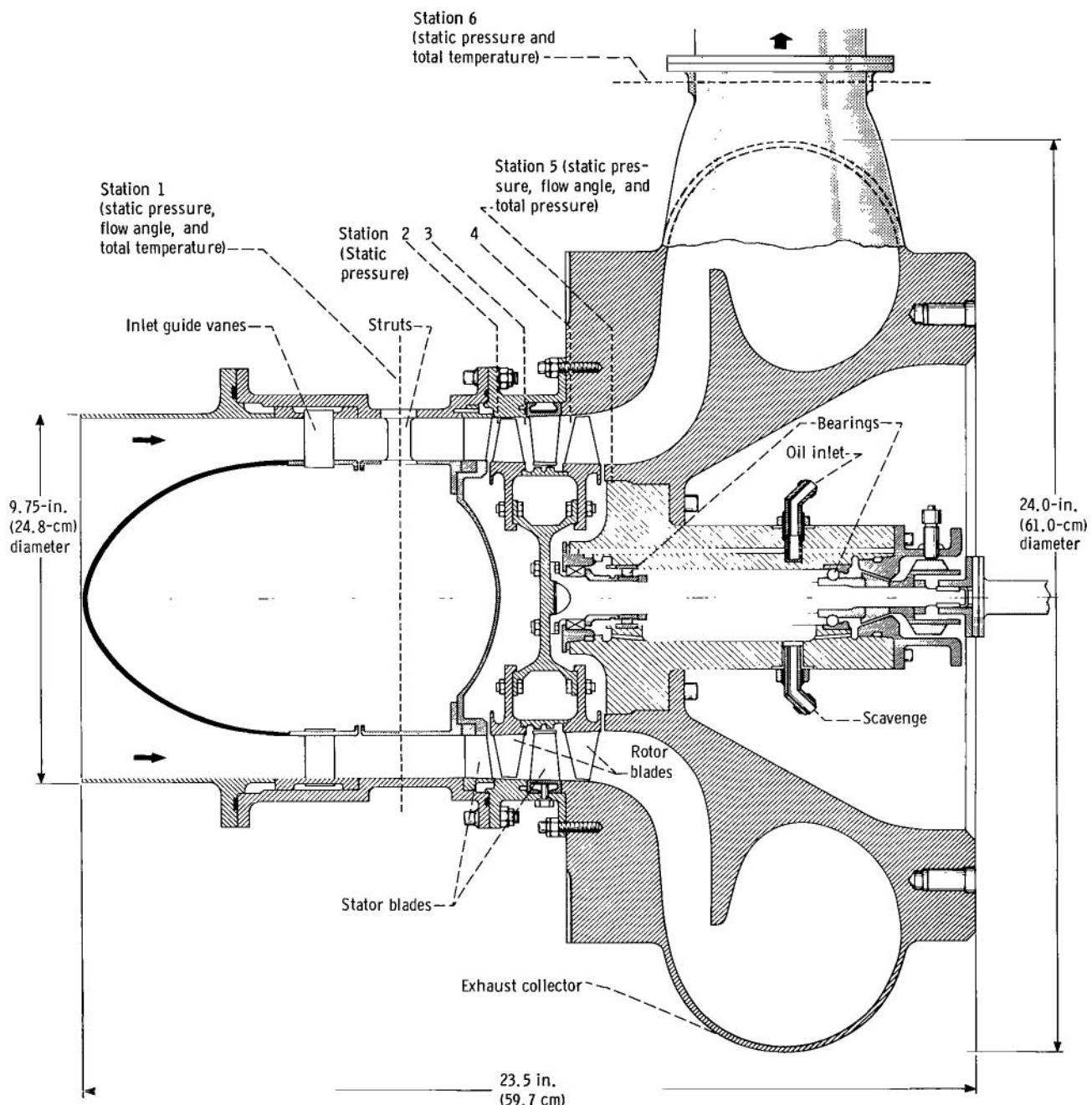
## Rotor Blading

The rotor design incorporated 36 blades in each of the two stages with tip diameters of 9.7 and 9.8 inches (24.6 and 24.9 cm) for the first and second stages, respectively. The resulting values of solidity at the mean diameter were 1.3 and 1.4. A low solidity (1.2) at the tip diameters together with a large amount of blade twist, as dictated by the velocity diagrams, resulted in a short guided channel in the tip region of the blade. This distinctive feature is seen in figure 2, which shows the rotor blade passages and profiles



C-66-3770

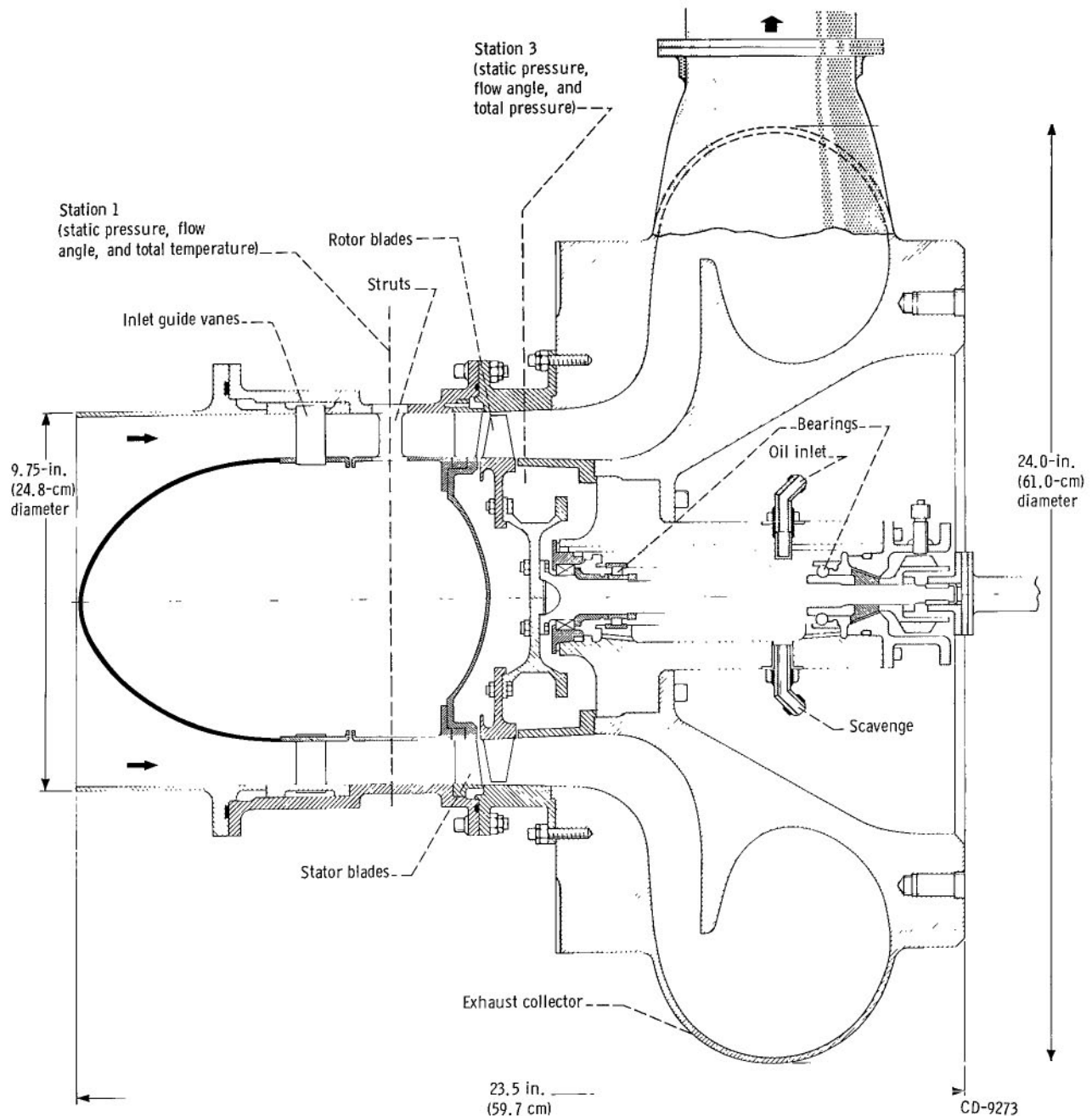
Figure 3. - Two-stage turbine rotor assembly.



(a) Two-stage operation.

CD-9272

Figure 4. - Cross section of turbine.



(b) First-stage operation.

Figure 4. - Concluded.

for both rotors. The large amount of blade twist is apparent in figure 3, which shows the rotor assembly. Rotor blade taper in both the axial chord and blade thickness, as shown in figure 2, is conducive to low blade stresses. The design blade-surface velocity distributions at the hub and mean diameters are presented in reference 4. There is generally accelerating flow from the inlet to the throat of both rotors with only a small amount of deceleration on the suction surface downstream of the throat. The decelerations were limited to small values in the blading design to increase the assurance of obtaining good blade performance, particularly in the low-Reynolds-number region encountered in this application.

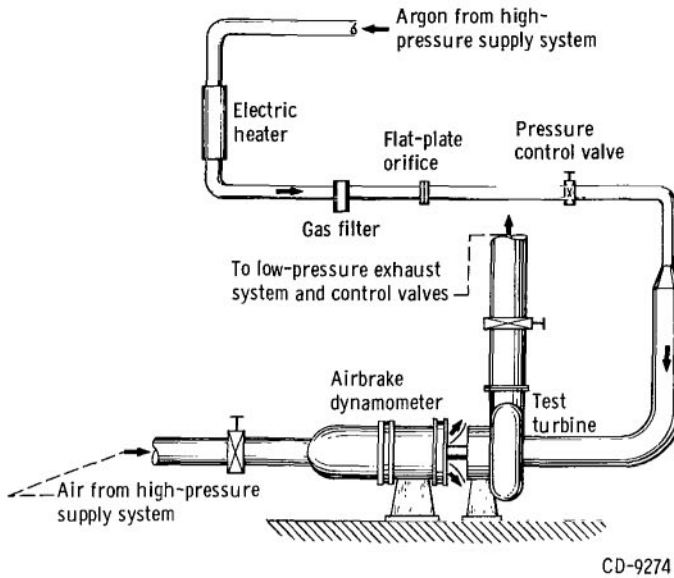
### Turbine Assembly

Figures 4(a) and (b) show cross-sectional views of the turbine for the two-stage and first-stage operations, respectively. The major dimensions of the turbine are given, as well as the arrangement of the blading, the gas flow passages, the bearings, and other details of the mechanical design. Included are 36 inlet guide vanes designed to give a prerotation to the flow of about  $12^{\circ}$  at the mean diameter, as stipulated by the velocity diagrams. Three struts afforded support for the inlet duct inner wall and also served as a path for the tubing connected to the static pressure taps in the inner wall.

Rotor blade tip clearances were 0.012 and 0.015 inch(0.030 and 0.038 cm) for the first and second stages, respectively. These values were approximately 1.0 and 1.1 percent of the blade heights. Both figures (4(a) and (b)) show the exhaust collector which includes the sharp radially outward turn in the flow passage immediately downstream of the blading. The rotating assembly was supported by a roller bearing and a ball bearing, which are jet-oil lubricated.

### APPARATUS, INSTRUMENTATION, AND PROCEDURE

The apparatus consisted of the turbine, described in the preceding section, an air-brake dynamometer to absorb and measure the power output of the turbine, and an inlet and exhaust piping system with flow controls. The arrangement of the apparatus is shown schematically in figure 5. Pressurized argon was used as the driving fluid for the turbine. The argon was piped into the turbine through an electric heater, a filter, a weight-flow measuring station consisting of a calibrated flat-plate orifice, and a remotely controlled pressure-regulating valve. The gas, after passing through the turbine, was exhausted through a system of piping and a remotely operated valve into the laboratory low-pressure exhaust system. With a fixed inlet pressure, the remotely operated valve in the exhaust line was used to obtain the desired pressure ratio across the turbine.



CD-9274

Figure 5. - Experimental equipment.

The airbrake dynamometer, which was cradle mounted on air bearings for torque measurement, absorbed and measured the power output of the turbine and at the same time, controlled the speed. The force on the torque arm was measured with a commercial strain-gage load cell. The rotational speed was measured with an electronic counter in conjunction with a magnetic pickup and a shaft-mounted gear. The turbine test facility is shown in figure 6.

The instrument measuring stations are shown in figure 4. Overall performance (flange to flange) for the two-stage operation (fig. 4(a)) was based on measurements taken at stations 1 and 6. Turbine performance was also determined by measurements taken at stations 1 and 5 (exit of the second-stage rotor). The following instrumentation was located at the turbine inlet (station 1): eight static pressure taps (four each on the inner and outer walls), a self-aligning probe for flow angle measurement, and two total-temperature rakes (each containing three thermocouples). At station 5, immediately downstream of the second-stage-rotor trailing edge, the instrumentation consisted of eight static pressure taps (four each at the inner and outer walls) and a self-aligning probe for flow angle, total-temperature, and total-pressure measurements. In the calculation of pressure ratio across the turbine, pressures at stations 1 and 5 were determined from the average of the static pressures at the inner and outer walls. Four static pressure taps and two total-temperature rakes were located at station 6. The temperature rakes were used primarily as a check on turbine efficiency as calculated from torque measurements. Interstage pressure taps were installed to determine the variation of

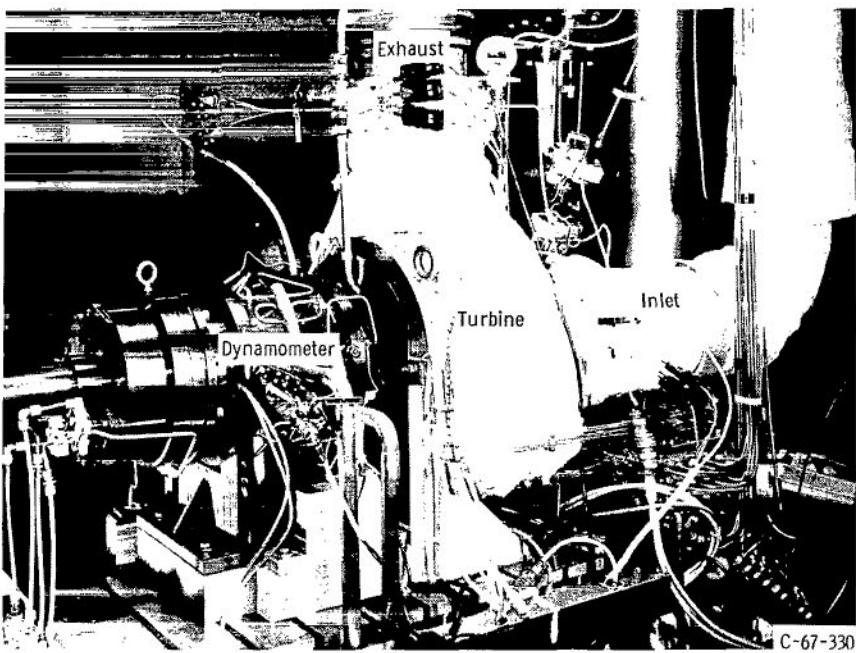


Figure 6. - Experimental turbine test setup.

static pressure through the turbine. Four static pressure taps were located in the outer wall at the exit of the first-stage stator (station 2), first-stage rotor (station 3), and second-stage stator (station 4).

Instrumentation for the first-stage operation (fig. 4(b)) was similar to that for the two-stage operation, except that stations 4 and 5 were eliminated and additional instrumentation was installed at station 3. In this case, performance was determined from measurements taken at station 1 and at the exit of the first-stage rotor (station 3). Instrumentation at station 3 for the first-stage operation consisted of eight static pressure taps (four each at the inner and outer walls) and a self-aligning probe for flow angle, total-temperature, and total-pressure measurements. Pressure ratio across the stage was determined from the average of the pressures measured at the inner and outer walls.

The absolute values of the pressures at the various stations were measured by the use of manometer tubes which contained a fluid of low specific gravity (1.04) and were evacuated to 10.0 microns of mercury ( $0.00013 \text{ newtons/cm}^2$ ) on the reference side of the manometer tube. All other data were recorded by an automatic digital potentiometer and processed through an electronic digital computer.

For both the two-stage and single-stage modes of operation, performance data were taken at nominal inlet total conditions of  $610.2^\circ \text{R}$  ( $339^\circ \text{K}$ ) and 2.5 psia ( $1.723 \text{ newtons/cm}^2$ ). These values of temperature and pressure correspond to a Reynolds number of about 47 400 at equivalent design speed and pressure ratio. This value of Reynolds

number is near the design value of 49 500. Reynolds number, as used herein, is defined as  $Re = w/\mu r_m$ . For the two-stage operation, data were taken over a range of equivalent inlet-total- to exit-static-pressure ratio ( $p'_1/p_5$ ) from about 1.08 to 1.66 and over a range of speeds from 0 to 120 percent of equivalent design speed. For the first-stage operation, data were taken over the same range of speed but at the slightly different range of equivalent pressure ratios of 1.05 to 1.56. For both modes of operation, a rotor-exit radial survey was made of flow angle, total pressure, and total temperature at equivalent design speed and pressure ratio.

Friction torque of the bearings and seals was obtained by measuring the amount of torque required to rotate the shaft and rotor over the range of speeds covered in the investigation. In measuring the friction torque, windage losses were minimized by evacuating the air from the turbine. A friction torque value of approximately 1.0 inch-pound (0.113 newton-meters) was obtained at equivalent design-point operation. This value corresponds to about 5.5 percent of two-stage turbine torque obtained at equivalent design rotative speed. Friction torque was added to shaft torque when turbine efficiency was determined.

The aerodynamic performance of the two-stage turbine was determined on the basis of both total and static efficiency from measurements taken at the turbine inlet (station 1) and second-stage rotor exit (station 5) (fig. 4(a)). Pressures at these stations were obtained from an average of the static pressures at the inner and outer walls. Overall performance of the turbine with exhaust-collector was obtained and then compared with that of the turbine in order to determine the effectiveness of the exhaust collector. The overall performance was based on both total and static efficiencies and was obtained from measurements taken at stations 1 and 6. First-stage performance was obtained from measurements taken as stations 1 and 3 (fig. 4(b)) where pressures at both stations were determined from an average of the static pressures at the inner and outer walls. The total pressures were calculated from weight flow, static pressure, total temperature, and flow angle from the following equation:

$$p' = p \left\{ \frac{1}{2} + \frac{1}{2} \left[ 1 + \frac{2(\gamma - 1)}{\gamma} \frac{R}{g} \left( \frac{w \sqrt{T'}}{pA \cos \alpha} \right)^2 \right]^{1/2} \right\}^{\gamma/\gamma-1}$$

In the calculation of total pressure at station 6, the flow was assumed to be normal to the plane defined by that station.

## RESULTS AND DISCUSSION

The results of this investigation are presented in two sections covering first-stage and two-stage performance, respectively. This performance was investigated at approximately design Reynolds number (at equivalent design speed and pressure ratio) with argon as the working fluid. All data, with the exception of the radial surveys, are shown in terms of equivalent air values. Experimental design-point performance results are given in table II, along with the values assumed in the design, to aid in the following discussion of results for both first-stage and two-stage performance.

TABLE II. - PERFORMANCE VALUES

	Operation			
	First-stage		Two-stage	
	Design	Experimental	Design	Experimental
Reynolds number, Re	49 500	46 900	49 500	47 700
Total efficiency, <sup>a</sup> $\eta_t$ , 1 to 3 (or 5)	0.847	0.867	<sup>b</sup> 0.850	0.845
Static efficiency, $\eta_s$ , 1 to 3 (or 5)	0.805	0.827	0.825	0.825
Overall total efficiency, $\eta_t$ , 1 to 6	-----	-----	0.843	0.835
Overall static efficiency, $\eta_s$ , 1 to 6	-----	-----	0.826	0.826
Equivalent specific work, $\Delta h/\theta_{cr}$ , Btu/lb (joules/gram)	2.98 (6.94)	3.07 (7.15)	5.96 (13.87)	5.96 (13.87)
Equivalent mass flow,	1.537 (0.697)	1.468 (0.666)	1.537 (0.697)	1.477 (0.670)
$\epsilon w \sqrt{\theta_{cr}/\delta}$ , lb/sec (kg/sec)				
Equivalent torque, $\tau \epsilon / \delta$ , in.-lb (newton-meters)	54.06 (6.11)	53.99 (6.10)	108.12 (12.22)	104.44 (11.80)

<sup>a</sup>Based on rotor-exit conditions.

<sup>b</sup>Based on total efficiencies of 0.847 for first and second stages.

### First-Stage Performance

Figure 7 shows the variation of the first-stage turbine specific work  $\Delta h/\theta_{cr}$  with total- to static-pressure ratio  $p_1/p_3$  for lines of constant speed. The specific work obtained at design speed and pressure ratio was 3.07 Btu per pound (7.15 joules/gram). This value is 3 percent greater than the design value of 2.98 Btu per pound (6.94 joules/gram). The low design pressure ratio of 1.112 indicates that the turbine had low subsonic internal velocity levels. The figure also shows that limiting loading was not reached over the range of pressure ratios investigated.

In figure 8, mass flow  $\epsilon w \sqrt{\theta_{cr}/\delta}$  is plotted against exit-static- to inlet-total-

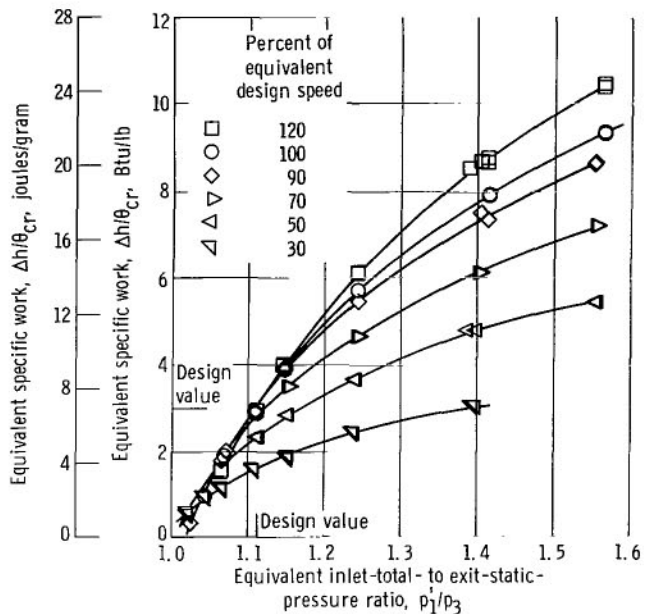


Figure 7. - Variation of specific work with pressure ratio and speed for first-stage operation.

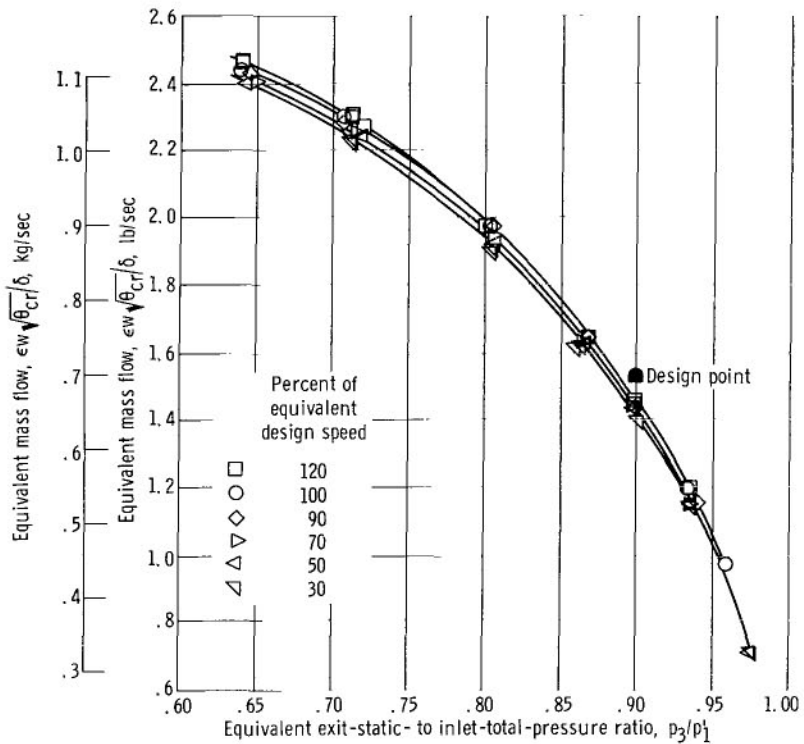


Figure 8. - Variation of mass flow with pressure ratio and speed for first-stage operation.

pressure ratio  $p_3/p'_1$  for lines of constant speed. At the design pressure ratio of 0.90, the mass flow was 1.468 pounds per second (0.666 kg/sec). This value is 4 percent lower than the design value of 1.537 pounds per second (0.697 kg/sec). Measurements of the first-stage stator and rotor throat areas indicated them to be smaller than the design values by 8 and 4 percent, respectively. Therefore, the deficiency in mass flow may be attributed to the smaller throat areas. The trends of the mass flow curves (i.e., the variation of mass flow with pressure ratio for lines of constant speed) are typical of subsonic turbines. The curves show that, for any given pressure ratio, mass flow increases with increasing speed.

The variation of torque  $\tau\epsilon/\delta$  with speed for lines of constant pressure ratio  $p'_1/p_3$  is shown in figure 9. These results are obtained from faired data because the

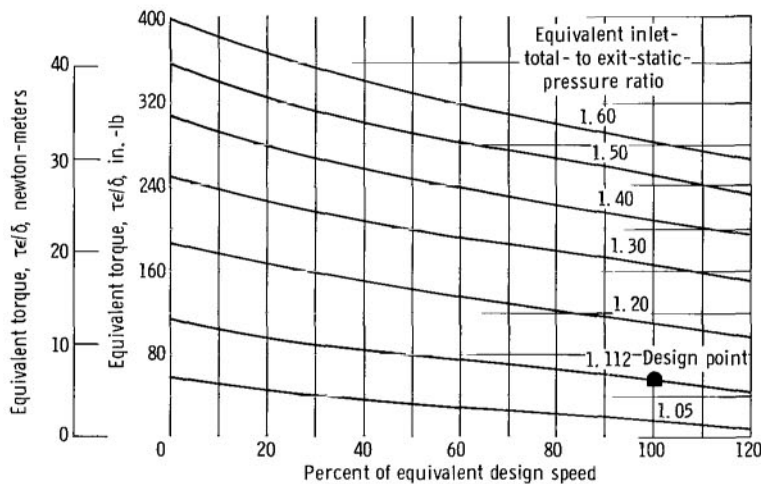
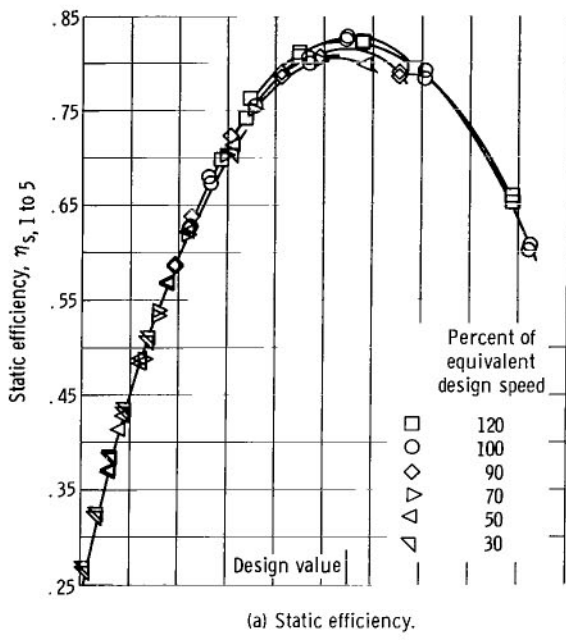


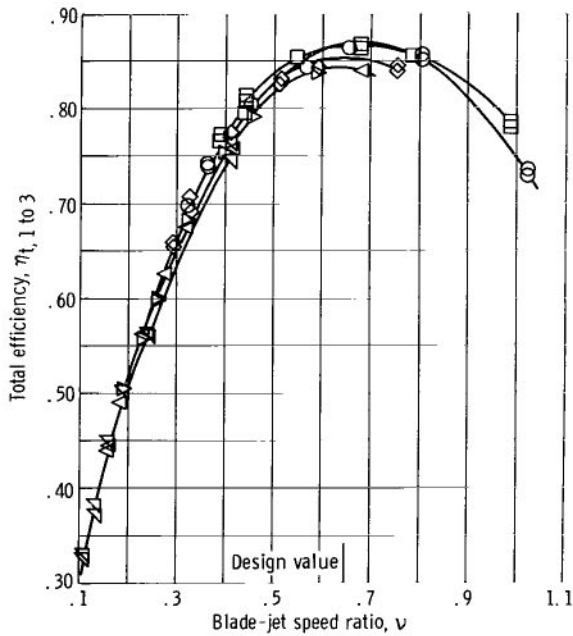
Figure 9. - Variation of torque with speed and pressure ratio for first-stage operation.

data were taken at constant blade speeds and not at constant pressure ratios. The torque at design speed and pressure ratio (1.112) was 53.99 inch-pounds (6.10 newton-meters) which is essentially equal to the design value of 54.06 inch-pounds (6.108 newton-meters). The attainment of design torque, coupled with the 4-percent decrease in mass flow, resulted in the increase in turbine specific work. The figure shows that zero speed torque, at design pressure ratio, is 112.40 inch-pounds (12.7 newton-meters), which is 2.1 times the value obtained at design speed and pressure ratio.

Figures 10 (a) and (b) present the static and total efficiencies of the first stage over the range of blade-jet speed ratios investigated. These figures show that the maximum efficiency occurs in the region of the design blade-jet speed ratio of 0.651. A static



(a) Static efficiency.



(b) Total efficiency.

Figure 10. - Variation of efficiency with blade-jet speed ratio for first-stage operation.

efficiency of 0.827 and a total efficiency of 0.867 were obtained at design speed and design total- to static-pressure ratio. These values are approximately 2 points higher than the respective design values of 0.805 and 0.847.

A radial survey of first-stage rotor-exit total pressure and rotor-exit flow angle was taken at design speed and pressure ratio. Figure 11 (a) shows the variation of exit total pressure with radius ratio. The dashed line represents design total- to total-pressure ratio. A region of comparatively low total pressure occurs near the hub at a radius ratio of about 0.77. Small deviations of total pressure from design value were obtained over the greater portion of the passage height. Hub and tip static pressures are plotted in the figure to indicate the low velocity level.

Figure 11 (b) shows large deviations in exit flow angle from design. The variation in flow angle and the low total pressure in the region near the inner wall suggest that this may be a core of low-momentum fluid. This fluid comes from the first stator in the region of the blade suction surface and the inner wall or from a redistribution of low-momentum accumulations in the rotor. Since the stator and rotor throat areas were smaller than design and the measured throat dimension did not vary in a uniform manner

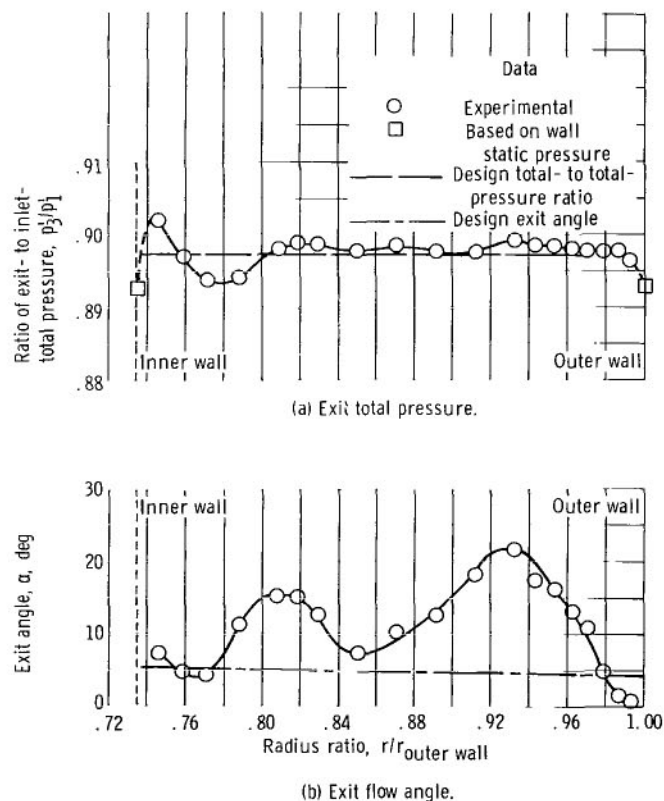


Figure 11. - Variation of rotor-exit total pressure and flow angle with radius ratio for first-stage operation at equivalent design speed and design pressure ratio.

from hub to tip, some deviations of exit flow angle over the passage height would also be expected.

Figure 11 (b) also shows that there was undeturning (as indicated by positive exit angles) over most of the radial distance. The combination of undeturning at the rotor exit and the attainment of specific work which was larger than design indicates that the whirl component at the rotor inlet was larger than design. This condition results from the stator blade angles being more tangential than design and in turn accounts for the flow area being smaller than design.

## Two-Stage Performance

As mentioned in APPARATUS, INSTRUMENTATION, AND PROCEDURE, two-stage turbine performance was determined by measurements taken at stations 1 and 5 (turbine inlet and rotor exit) and at stations 1 and 6 (turbine inlet and exit of collector). Efficiency based on measurements at stations 1 and 5 gives the performance of the turbine to the rotor exit. Efficiency based on measurements at stations 1 and 6 gives an overall turbine performance which is of importance for the space power system since the exit collector is part of the turbine package for the system. Blade-jet speed ratio, in all

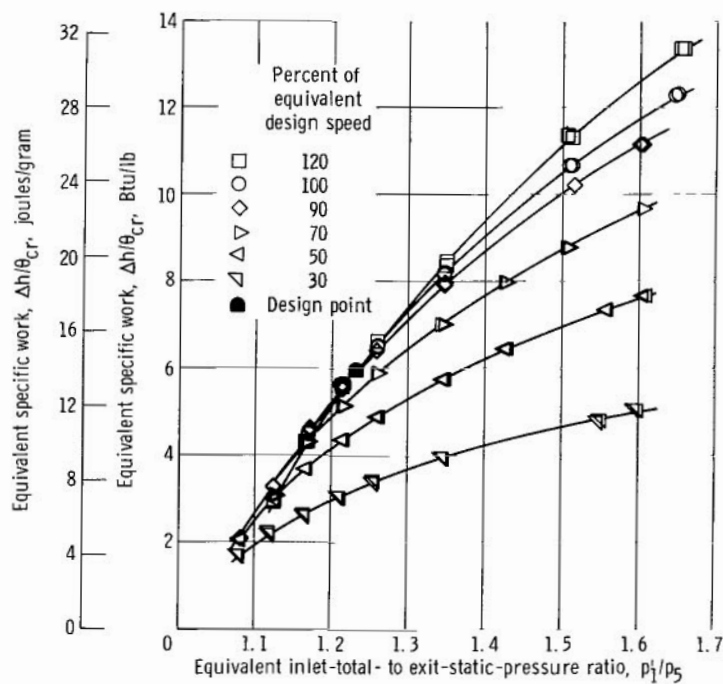


Figure 12. - Variation of specific work with pressure ratio and speed for two-stage operation.

cases, was based on conditions at the turbine inlet and the rotor exit.

The variation of specific work  $\Delta h/\theta_{cr}$  with pressure ratio  $p_1'/p_5$  and speed is shown in figure 12. A specific work value of 5.96 Btu per pound (13.87 joules/gram) was obtained at design speed and pressure ratio. This value agrees with the design value of 5.96 Btu per pound (13.87 joules/gram). For the speed range of 90 to 120 percent of design, turbine work was constant in the region of design pressure ratio, which indicates a constant efficiency region. The curves show that, for the pressure ratio range investigated, limiting loading was not reached.

Mass flow  $\epsilon w \sqrt{\theta_{cr}/\delta}$  is plotted against rotor exit-static- to inlet-total-pressure ratio  $p_5/p_1'$  in figure 13 for lines of constant speed. At design pressure ratio (0.811) and speed, the mass flow was 1.477 pounds per second (0.670 kg/sec). This value is 4 percent lower than the design value of 1.537 pounds per second (0.697 kg/sec). This deficiency in mass flow is again attributed to the throat areas of all stators and rotors being somewhat smaller than design. The variation of mass flow with pressure ratio for lines of constant speed is typical of turbines of subsonic design.

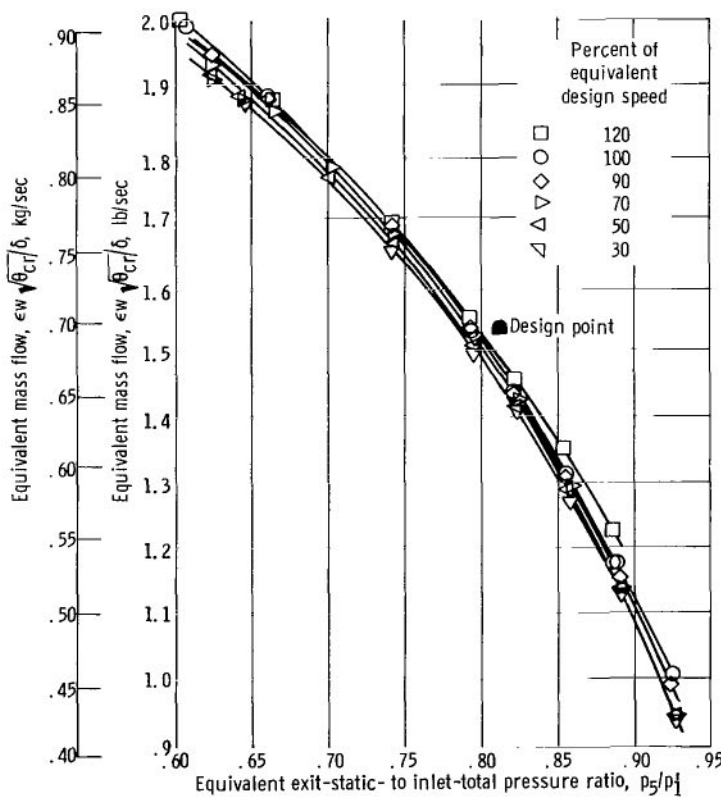


Figure 13. - Variation of mass flow with pressure ratio and speed for two-stage operation.

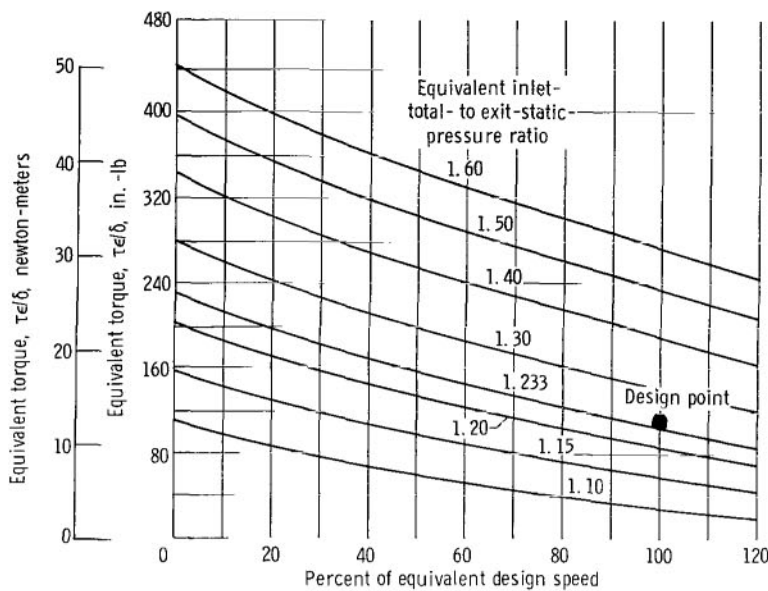
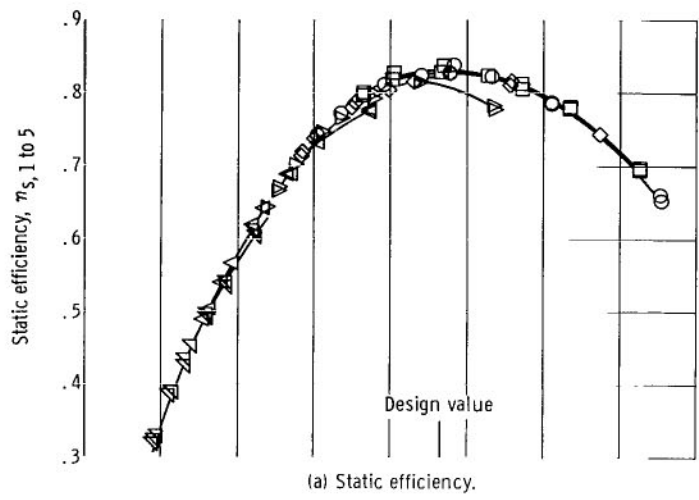


Figure 14. - Variation of torque with speed and pressure ratio for two-stage operation.

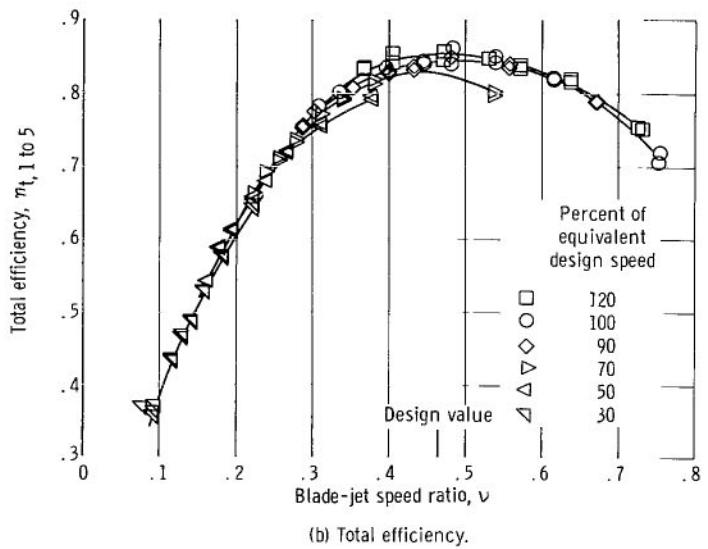
The variation of torque  $\tau_e / \delta$  with speed and pressure ratio is shown in figure 14. A torque value of 104.44 inch-pounds (11.80 newton-meters) was obtained at design speed and at a pressure ratio of 1.233. This torque value is 3.5 percent lower than the design value of 108.12 inch-pounds (12.22 newton-meters). Since specific work was equal to design value and the mass flow was 4 percent lower than design, the torque would be expected to be smaller than design. The slight upward trend of the torque-speed curves as speed is reduced is typical of curves obtained for two-stage axial-flow turbines. A zero-speed torque value of 231.1 inch-pounds (26.11 newton-meters) was obtained at design pressure ratio. This torque is 2.2 times that obtained at design speed and pressure ratio.

Figure 15 shows the performance of the turbine from inlet to rotor exit in terms of static and total efficiencies. Figure 15(a) indicates that design static efficiency  $\eta_{s,1 \text{ to } 5}$  of 0.825 was obtained at design speed and at a design blade-jet speed ratio of 0.465. The curves show that the efficiency is not affected by speed for speeds over 90 percent of design. Figure 15 (b) shows that a total efficiency  $\eta_{t,1 \text{ to } 5}$  of 0.845 was obtained at design speed and design blade-jet speed ratio. This value is only slightly lower than the design value of 0.850.

Figure 16 shows the overall turbine performance which includes the turbine exit collector. Figure 16 (a) indicates that design static efficiency  $\eta_{s,1 \text{ to } 6}$  of 0.826 was obtained at design speed and design blade-jet speed ratio. Figure 16(b) indicates that the associated total efficiency  $\eta_{t,1 \text{ to } 6}$  was 0.835 at design speed and design blade-jet

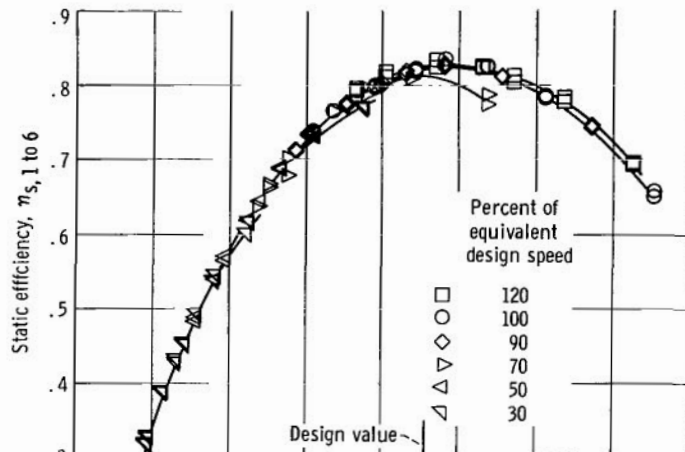


(a) Static efficiency.

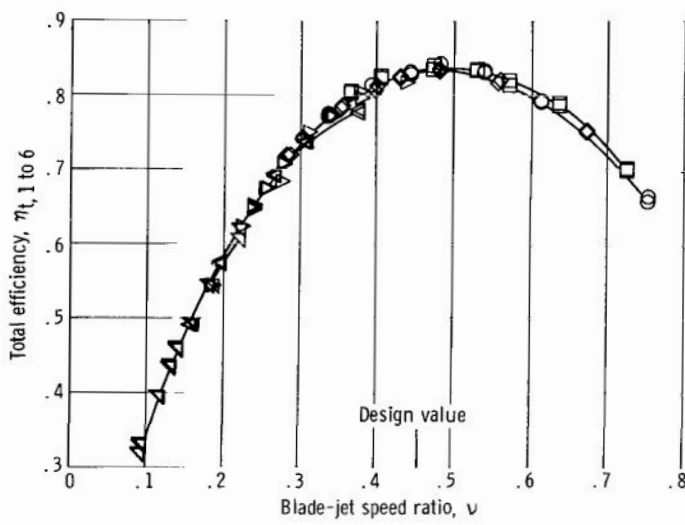


(b) Total efficiency.

Figure 15. - Variation of efficiency with blade-jet speed ratio for two-stage operation (based on rotor-exit conditions).



(a) Static efficiency.



(b) Total efficiency.

Figure 16. - Variation of overall efficiency with blade-jet speed ratio for two-stage operation (based on collector-exit conditions).

speed ratio. This value of efficiency is 0.8 point lower than the design value of 0.843. Comparison of static efficiencies obtained at the rotor exit with those at the collector exit, for design speed and pressure ratio, shows that there was little static pressure recovery through the collector. In addition, comparison of total efficiencies shows that there was a drop of about 1 point in total efficiency through the collector. These experimental values are the same as the design values, and hence the collector performed as designed.

Figure 17 shows the variation of tip static pressure through the turbine at design

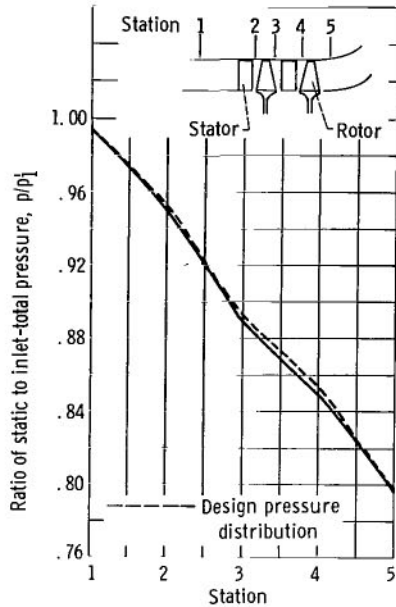


Figure 17. - Variation of tip static pressure through turbine at equivalent design speed and design pressure ratio.

speed and pressure ratio. Comparison of the experimental static pressure variation with design shows that approximately design reaction was obtained across all blade rows.

For two-stage operation at design speed and pressure ratio, the first-stage was operating at a rotor-exit-tip-static- to inlet-total-pressure ratio of 0.889. With this pressure ratio and the results from first-stage and two-stage performance data, the work split for two-stage operation was 3.15 Btu per pound (7.33 joules/gram) for the first stage and 2.81 Btu per pound (6.55 joules/gram) for the second stage, which represents a stage work split of 53 to 47. The turbine was designed for an equal work split of 2.98 Btu per pound (6.937 joules/gram) per stage. Based on the two-stage total efficiency (based on rotor-exit conditions) of 0.845 and the measured first-stage total efficiency of 0.864, the associated second-stage total efficiency was computed to be 0.805, which is approximately 4 points lower than design.

The radial variation of rotor-exit total pressure and flow angle for two-stage operation is shown in figure 18 for design speed and design total- to static-pressure ratio. The trends shown in this figure are similar to those obtained at the first-stage rotor exit, as described in figure 11, with the general undeturning at the exit again indicated.

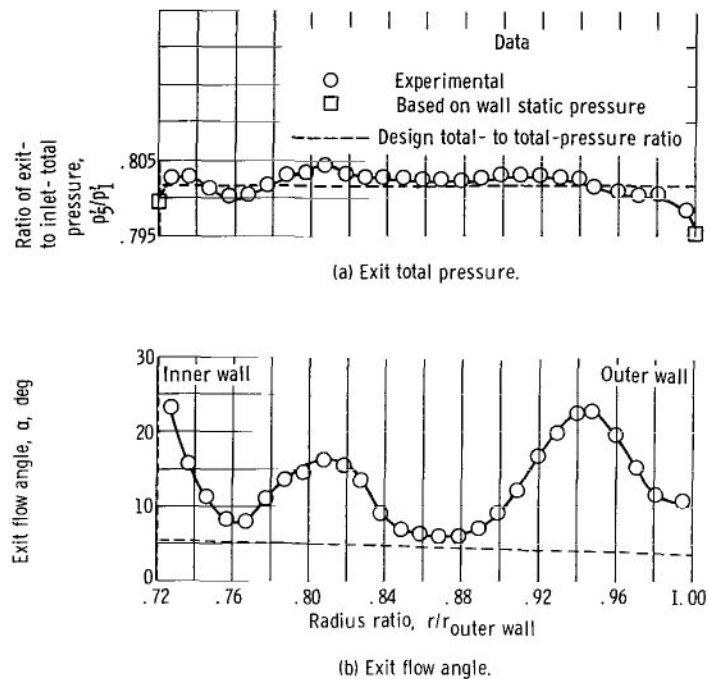


Figure 18. - Variation of rotor-exit total pressure and flow angle with radius ratio for two-stage operation at equivalent design speed and design pressure ratio.

## SUMMARY OF RESULTS

An experimental investigation of a two-stage axial-flow turbine with a mean diameter of 8.50 inches (21.59 cm) was conducted to determine the performance at design Reynolds number. This turbine was designed to drive a low-speed alternator for a 10-kilowatt-shaft-output space power system. Performance characteristics were obtained for both first-stage and two-stage operation. The results of this investigation are summarized as follows:

1. An equivalent specific work of 5.96 Btu per pound (13.88 joules/gram) was obtained for two-stage operation at design speed and inlet-total- to rotor-exit-static-pressure ratio. The associated static and total efficiencies (based on turbine-inlet and rotor-exit conditions) were 0.825 and 0.845, respectively, which compare favorably with design.
2. At this design point the flow was 1.477 pounds per second (0.670 kg/sec). This value was 4 percent lower than design and resulted principally from the flow areas in the blade rows being smaller than design since approximate design reaction was obtained.
3. Two-stage performance based on turbine-inlet and collector-exit conditions indicated static and total efficiencies of 0.826 and 0.835, respectively. These results indi-

cate a drop of approximately 1 point in total efficiency within the collector with no change in static efficiency and again agree closely with design.

4. Results of the first-stage tests indicated static and total efficiencies of 0.827 and 0.867, which were approximately 2 points greater than design. This improved first-stage performance resulted in an indicated second-stage total efficiency of 0.805, which is approximately 4 points less than design. As a result, a stage work split of 53 to 47 was indicated compared with a design equal split.

Lewis Research Center,  
National Aeronautics and Space Administration,  
Cleveland, Ohio, September 18, 1967,  
120-27-03-13-22.

## APPENDIX - SYMBOLS

A	flow area in. <sup>2</sup> (cm <sup>2</sup> )
g	gravitational constant, 32.174 ft/sec <sup>2</sup>
Δh	specific work, Btu/lb (joules/gram)
J	mechanical equivalent of heat, 778.029 (ft-lb)/Btu
N	turbine speed, rpm
p	absolute pressure, psi (newton/cm <sup>2</sup> )
R	gas constant (ft-lb)/(lb)( <sup>0</sup> R)(newton-meter/(kg)( <sup>0</sup> K))
Re	Reynolds number, w/μr <sub>m</sub>
r	radius, ft (m)
T	absolute temperature, <sup>0</sup> R ( <sup>0</sup> K)
U	blade velocity, ft/sec (m/sec)
V	absolute gas velocity, ft/sec (m/sec)
V <sub>j</sub>	ideal jet speed corresponding to total- to static-pressure ratio across turbine, ft/sec (m/sec)
W	relative gas velocity, ft/sec (m/sec)
w	mass flow, lb/sec (kg/sec)
α	absolute gas flow angle measured from axial direction, deg
γ	ratio of specific heats
δ	ratio of inlet-total pressure to U.S. standard sea-level pressure
ε	function of γ used in relating parameters to those using air inlet conditions at U.S. standard sea-level conditions,

$$\frac{\gamma^*}{\gamma} \left[ \frac{\left( \frac{\gamma + 1}{2} \right)^{\gamma/\gamma-1}}{\left( \frac{\gamma^* + 1}{2} \right)^{\gamma^*/\gamma^*-1}} \right]$$

η <sub>s</sub>	static efficiency (based on inlet-total- to exit-static-pressure ratio)
η <sub>t</sub>	total efficiency (based on inlet-total- to exit-total-pressure ratio)
θ <sub>cr</sub>	squared ratio of critical velocity at turbine inlet to critical velocity at U.S. standard sea-level temperature, (V <sub>cr</sub> /V <sub>cr</sub> <sup>*</sup> ) <sup>2</sup>

$\mu$  gas viscosity, lb/(ft)(sec) (Kg/(m)(sec))

$\nu$  blade-jet speed ratio,  $U_m/V_j$

$\tau$  torque, in.-lb (newton-meter)

Subscripts:

cr condition corresponding to Mach 1

eq air equivalent (U.S. standard sea level)

id ideal

m mean radius

1 station at turbine inlet

2 station at first-stage stator exit

3 station at first-stage rotor exit

4 station at second-stage stator exit

5 station at second-stage rotor exit

6 station at exhaust-pipe flange

Superscripts:

' absolute total state

\* U. S. standard sea-level conditions (temperature,  $518.67^{\circ}$  R ( $288.15^{\circ}$  K);  
pressure, 14.696 psia ( $10.128 \text{ newton/cm}^2$ ))

## REFERENCES

1. Bernatowicz, Daniel T.: NASA Solar Brayton Cycle Studies. Paper presented at the Symposium on Solar Dynamics Systems, Interagency Advanced Power Group, Washington, D. C., Sept. 24-25, 1963.
2. Kofskey, Milton G; and Holeski, Donald E.: Cold Performance Evaluation of a 6.02-Inch Radial Inflow Turbine Designed for a 10-kilowatt Shaft Output Brayton Cycle Space Power Generation System. NASA TN D-2987 (Rev.) 1966.
3. Holeski, Donald E.; and Futral, Samuel M., Jr.: Experimental Performance Evaluation of a 6.02-Inch Radial-Inflow Turbine Over a Range of Reynolds Number. NASA TN D-3824, 1967.
4. Cohen, R.; Gilroy, W. K.; and Havens, F. D.: Turbine Research Package for Research and Development of High Performance Turboalternator. Rep. No. PWA-2796 (NASA CR-54885), Pratt and Whitney Aircraft, Jan. 1967.
5. Forrette, Robert E.; Holeski, Donald E.; and Plohr, Henry W.: Investigation of the Effects of Low Reynolds Number Operation on the Performance of a Single-Stage Turbine with a Downstream Stator. NASA TM X-9, 1959.
6. Cohen, R.; Gilroy, W. K.; and Havens, F. D.: Turbine Research Package for Research and Development of High Performance Axial Flow Turbine-Compressor. Rep. No. PWA-2822 (NASA CR-54883), Pratt and Whitney Aircraft, Dec. 1966.

National Aeronautics and Space Administration

WASHINGTON, D. C.

OFFICIAL BUSINESS

FIRST CLASS MAIL

POSTAGE AND FEES PAID  
NATIONAL AERONAUTICS AND  
SPACE ADMINISTRATION

04U 001 28 51 3DS 00903  
AIR FORCE WEAPONS LABORATORY/AFWL/  
KIRTLAND AIR FORCE BASE, NEW MEXICO 87117

ATT MISS MADELINE F. LANDUA, CHEF TECHNICIAN  
LIBRARY / ALIBI

POSTMASTER: If Undeliverable (Section 158  
Postal Manual) Do Not Return

*"The aeronautical and space activities of the United States shall be conducted so as to contribute . . . to the expansion of human knowledge of phenomena in the atmosphere and space. The Administration shall provide for the widest practicable and appropriate dissemination of information concerning its activities and the results thereof."*

—NATIONAL AERONAUTICS AND SPACE ACT OF 1958

## NASA SCIENTIFIC AND TECHNICAL PUBLICATIONS

**TECHNICAL REPORTS:** Scientific and technical information considered important, complete, and a lasting contribution to existing knowledge.

**TECHNICAL NOTES:** Information less broad in scope but nevertheless of importance as a contribution to existing knowledge.

**TECHNICAL MEMORANDUMS:** Information receiving limited distribution because of preliminary data, security classification, or other reasons.

**CONTRACTOR REPORTS:** Scientific and technical information generated under a NASA contract or grant and considered an important contribution to existing knowledge.

**TECHNICAL TRANSLATIONS:** Information published in a foreign language considered to merit NASA distribution in English.

**SPECIAL PUBLICATIONS:** Information derived from or of value to NASA activities. Publications include conference proceedings, monographs, data compilations, handbooks, sourcebooks, and special bibliographies.

**TECHNOLOGY UTILIZATION PUBLICATIONS:** Information on technology used by NASA that may be of particular interest in commercial and other non-aerospace applications. Publications include Tech Briefs, Technology Utilization Reports and Notes, and Technology Surveys.

*Details on the availability of these publications may be obtained from:*

SCIENTIFIC AND TECHNICAL INFORMATION DIVISION  
NATIONAL AERONAUTICS AND SPACE ADMINISTRATION

Washington, D.C. 20546